After 6 days of co-culture, hematopoietic progenitors were detected only on the A54 cells. These results suggest that only A54 cells have the ability to support hematopoietic cell growth among these three cell lines, consistent with the previous report. Hematopoietic cell proliferation was not observed on the layer of the terminally differentiated A54 adipocytes, suggesting that A54 cells lose the ability for hematopoietic cell support after adipocyte differentiation. To understand the molecular mechanisms of this observation, we examined the expression levels of SCF, SDF-1, and Ang-1 during adipocyte differentiation by RT real-time PCR. The expression levels of Ang-1 and SCF decreased immediately after the induction of adipocyte differentiation, and that of SDF-1 decreased gradually. In contrast to this, the level of adipocyte differentiation marker, CEBP-δ, was unchanged.

The analysis of functionally unknown molecules is currently underway. In addition, cell-to-cell contact is also believed to be crucial in the interaction between hematopoietic stem cells and MSCs. We are currently investigating the cellular and molecular events in the interactive communication between hematopoietic stem cells and MSCs.

3. Nitric oxide (NO) plays a critical role in suppression of T-cell proliferation by mesenchymal stem cells

There is a case report of severe steroid-resistant GVHD after bone marrow transplantation, in which intravenous infusion of MSCs greatly improved clinical manifestations [3]. Moreover, multi-institutional clinical trial of MSC-treatment of severe grade III–IV acute GVHD in Europe revealed very high overall response rate (about 70%) (Le Blanc et al., ASH meeting 2006). The molecular mechanisms by which MSCs suppress T-cell proliferation are complicated, and whether a soluble factor plays a major role remains controversial. Transforming growth factor-β (TGF-β), hepatocyte growth factor (HGF), indoleamine 2,3-dioxygenase (IDO), and prostaglandin E_2 (PGE_2) have been reported to mediate T-cell suppression by MSCs [15–17]. In addition, some reports have shown that a soluble factor is the major mediator of suppression, whereas some reports have demonstrated that T-cell-MSC contact is required for this suppression.

We also investigated the molecular mechanisms using primary murine MSCs, and focused on nitric oxide (NO), because it is known to inhibit T-cell proliferation. NO is produced by NO synthases (NOSs), of which there are 3 subtypes; i.e. inducible NOS (iNOS), endothelial NOS, and neuronal NOS. It has been known that macrophages suppress T-cell proliferation, and that this suppression is caused by NO-mediated inhibition of Stat5 phosphorylation [18]. We investigated whether MSCs can also produce NO and whether NO is involved in their ability to suppress T-cell proliferation [19].

T cells proliferated in response to PMA and ionomycin, which act downstream of the T-cell-receptor complex by activating protein kinase C and inducing Ca^{2+} influx, respectively. Such T-cell proliferation was suppressed by the presence of MSC, suggesting that MSCs influence signals downstream of protein kinase C and Ca^{2+} influx. The expression of the activation markers CD25 and CD69 on CD4 or CD8 T cells did not change even in the presence of MSCs. MSCs suppressed the production of IFN-γ but not IL-2.

Although T cells from $Stat5^{-/-}$ mice do not proliferate upon stimulation with anti-CD3, they up-regulate CD25. Because this phenotype is similar to the status of activated T cells in the presence of MSCs, we hypothesized that MSCs suppress Stat5 phosphorylation. Indeed, Stat5 phosphorylation in activated T cells was diminished in the presence of MSCs. We found that MSCs caused a significant and cell-dose-dependent production of NO only when co-cultured with activated T cells. The induction of iNOS was readily detected in MSCs but not in T cells. RT-PCR and Western blot analysis detected iNOS expression in MSCs cocultured with activated splenocytes but not in MSCs or splenocytes when cultured alone. The immunofluorescence studies showed that iNOS was exclusively expressed in $CD45^-$ adherent cells, which correspond to MSCs, but not in $CD45^+$T cells. Next, we investigated the effects of *N*-nitro-L-arginine methyl ester (L-NAME), a specific inhibitor of NOS. As expected, L-NAME dose-dependently inhibited the production of NO by MSCs in the presence of activated T cells. Importantly, L-NAME restored T-cell proliferation and Stat5 phosphorylation, indicating that NO is involved in the inhibition of T-cell proliferation and Stat5 phosphorylation. Moreover, MSCs from inducible $NOS^{-/-}$ mice had a reduced ability to suppress T-cell proliferation.

In the presence of direct interaction between T cells and MSCs, there was a high level of NO production accompanied by a strong suppression of T-cell proliferation. In contrast, both NO production and T-cell suppression were reduced in a transwell system, in which T cells were separated from MSCs by a 1-μm-pore membrane. There are two possible explanations for the difference in T-cell suppression between the presence and absence of the transwell system. First, the amount of NO produced in the transwell system was lower than that in the presence of direct interaction. This finding suggests that direct interaction is critical for efficient production of NO as well as for strong suppression of T-cell proliferation. A second possible explanation is that, because NO is highly unstable, it can lose its activity before it reaches T cells in the transwell system.

Because TGF-β, IDO, and PGE_2 were reported as mediators of T-cell suppression by MSCs, we compared the effects of L-NAME with inhibitors of each mediator. Indomethacin (inhibitor of PGE_2 production) but not 1-methyl-DL-tryptophan (1-MT: inhibitor of IDO) or an anti-TGF-β-neutralizing antibody restored T-cell proliferation as effectively as L-NAME; however, the effects of L-NAME and indomethacin were not additive, suggesting that the NO and PGE_2 share signaling pathways leading to T-cell suppression.

In summary, our hypothesis that NO is produced by MSCs and that it suppresses T-cell proliferation in part through inhibition of Stat5 phosphorylation was supported by the following facts: (1) NO was readily detected in the medium in the co-culture of MSCs and activated T cells; (2) L-NAME restored T-cell proliferation as well as Stat5 phosphorylation; and (3) MSCs from $iNOS^{-/-}$ mice had markedly

reduced ability to suppress T-cell proliferation. This hypothesis was further confirmed by the finding that iNOS expression was detected only in MSCs co-cultured with activated T cells.

In our scenario (Fig. 2), when MSCs are administered to the patients with severe acute GVHD, MSCs are considered to accumulate at the site of inflammation. Upon interaction with activated T cells, MSCs express iNOS and produce NO, which suppresses T-cell proliferation via inhibition of STAT5 phosphorylation. Systemic adverse effects of NO do not occur due to local production of NO with very short half-life. This is a very important point, because conventional treatment of acute GVHD causes severe systemic immunosuppression, which sometimes leads to life-threatening infections. Since MSC treatment causes just local immunosuppression, it should be much safer.

4. Interferon-γ and NF-κB mediate nitric oxide production by mesenchymal stem cells

Human MSCs were reported to suppress Th1 differentiation and augment Th2 differentiation. Therefore, we investigated whether mouse bone-marrow-derived MSCs and the 10T1/2 cell lines have the same effect on Th1 and Th2. We found a reverse correlation between NO production and T cell proliferation in Th1/Th2 conditions, where NO production was highly induced in the presence of MSCs in Th1 but it was only minimally induced in Th2. In particular, primary MSCs and the A54 preadipocyte cell line, which induce strong T cell suppression in Th1, produce high levels of NO in Th1 condition. These results suggest that NO also plays a major role in the preferential suppression of Th1 proliferation by MSCs.

To determine what inhibits the production of NO in Th2 condition, the two differentiation factors that support Th2 differentiation, anti-IFN-γ antibody and IL-4, were investigated. As a result, anti-IFN-γ antibody clearly inhibited the production of NO, whereas suppression by IL-4 was less evident. These results suggest that IFN-γ is a key regulator of NO production by MSCs.

Interestingly, cell supernatant collected from activated T cells had the ability to induce NO production by MSCs. IFN-γ is critical for NO production; however, in a T cell-free environment, IFN-γ alone does not induce NO production from primary MSCs. IFN-γ in combination with LPS, but not IL-2, stimulates NO secretion from primary MSCs, suggesting that both the IFN-γ and the signal from Toll-like receptor-4 (TLR4) are required for NO induction by MSCs. The addition of flagellin induced NO production in combination with IFN-γ. While, synthetic double strand RNA, poly(I:C), and CpG-oligonucleotide did not induce NO. Flagellin is a protein component of bacteria known to induce NO production from macrophages via TLR5 in the presence of either a TLR4 or IFN-γ signal. In addition to these factors, IL-1β and TNF-α induce NO when provided in combination with IFN-γ. As NF-κB is a downstream target of the signaling cascades activated by LPS, flagellin, IL-1β, and TNF-α, we hypothesized that activation of NF-κB is required for NO induction by MSCs. Bay-11-7085, a specific inhibitor of NF-κB, suppressed induction of iNOS in MSCs, thus suggesting that NF-κB is involved in NO production by MSCs as well as IFN-γ [20].

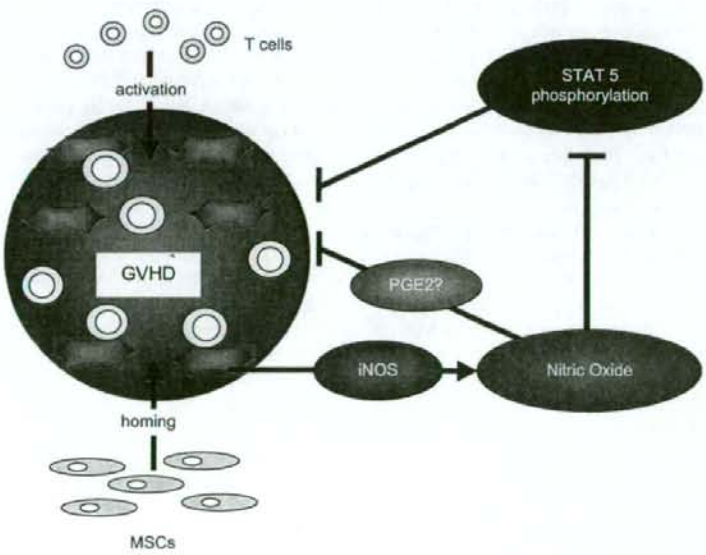

Fig. 2. MSC treatment of acute GVHD and the molecular mechanisms of T-cell suppression. MSCs are considered to accumulate at the site of inflammation and systemic adverse effects may not appear due to the local production of NO, which has very short half-life.

5. Retroviral vector-producing mesenchymal stem cells for tumor tracking and therapeutic gene amplification in suicide cancer gene therapy

MSCs are known to have a tendency to accumulate at the site of tumors, and therefore can be utilized as a platform for targeted delivery of anti-cancer agents [21–23]. The MSC-based targeted cancer gene therapy can enhance the therapeutic efficacy, because MSCs are considered to reach tumors including metastatic lesions and to deliver therapeutic molecules in a concentrated fashion. This targeted therapy can also reduce systemic adverse side effects, because the anti-cancer agents act locally at the site of tumors without elevating their systemic concentrations. We developed genetically-modified MSCs that produce retroviral vectors encoding HSV*tk*, aiming at augmenting therapeutic efficacy of systemic suicide cancer gene therapy (Fig. 3). The tumor tropism and anti-tumor effects of vector-producing MSCs (VP-MSCs) were examined by intravascular injection in tumor-bearing nude mice. MSCs isolated from the bone marrow of SD rats were transfected with plasmid DNA expressing luciferase alone (=non-VP-MSCs) or whole retroviral vector components (LTR-Luc or LTR-HSV*tk* with Gag-pol and VSV-G) (=VP-MSCs) by nucleofection. To assess tumor tropism of MSCs, nude mice were subcutaneously inoculated with 9 L rat glioma cells or Rat-1 fibroblasts, and were subsequently injected with luciferase-expressing MSCs through the left ventricular cavity. The transgene expression was periodically traced by using an *in vivo* imaging system. As a result, the transgene expression accumulated at the site of subcutaneous 9 L tumors, but undetectable at the site of Rat-1 fibroblasts. In addition, the injection of luciferase-expressing VP-MSCs caused much stronger signal of bioluminescence at the site of 9 L tumors compared with luciferease-expressing non-VP-MSCs. Immunostaining study showed that luciferase-positive cells (injected MSCs and transduced glioma cells) were detected at the periphery of tumors. To evaluate the therapeutic efficacy, tumor-bearing nude mice were treated with non-VP-MSCs or VP-MSCs combined with HSV*tk*/GCV system and then the size of subcutaneous tumors was periodically measured. In this model experiments, tumor growth was more efficiently suppressed by injecting VP-MSCs compared with non-VP-MSCs (Uchibori R, et al.: manuscript in preparation). This study suggests the effectiveness of VP-MSCs in suicide cancer gene therapy. The therapeutic benefit of this strategy should be further examined in orthotopic and metastatic tumor models.

6. Site-specific insertion of a therapeutic gene into the AAVS1 locus (19q13.4) in human mesenchymal stem cells by using adeno-associated virus integration machinery

Hematopoietic stem cells, ES cells, and MSCs are attractive targets for gene therapy and regenerative medicine, since they replicate themselves and differentiate into various cell lineages. To introduce genes in these stem cells, it is especially important to utilize a system that results in a minimal risk of insertional mutagenesis. To date, only one animal virus, the adeno-associated virus (AAV), is able to integrate into a defined site in human chromosome, AAVS1 (19q13.4), which is mediated by the activity of specific replicase/integrase protein, Rep. The Rep78 or Rep68 protein recognizes the GAGC motif on the viral inverted terminal repeat (ITR) sequence and a similar motif in AAVS1, leading to the site-specific integration of the AAV genome.

We and others have reported that a plasmid transfection system utilizing AAV derived components, the *rep* gene and ITR, could integrate the gene of interest preferentially into AAVS1 in epithelial or adherent cells (e.g., 293, HeLa, Huh-7 cells) [24–26]. Our system uses two plasmids, one harboring the transgene cassette flanked by the ITR sequences, and the other for *rep* expression, allowing only plasmid DNA harboring the ITR to integrate into the AAVS1 locus. In addition, this system can deliver DNA segments larger than the 4.5-kb packaging limit of AAV. As a first step toward establishing a method capable of integrating therapeutic DNA into the AAVS1 locus in MSCs, we tested this strategy in KM-102 cells, a cell line derived from human marrow stromal cells. KM-102 cells were co-transfected with a bicistronic plasmid containing a humanized GFP gene and a blasticidin S resistance gene (*bsr*) between the ITRs and a Rep68 plasmid. After transfection, single cell clones were grown in the presence of

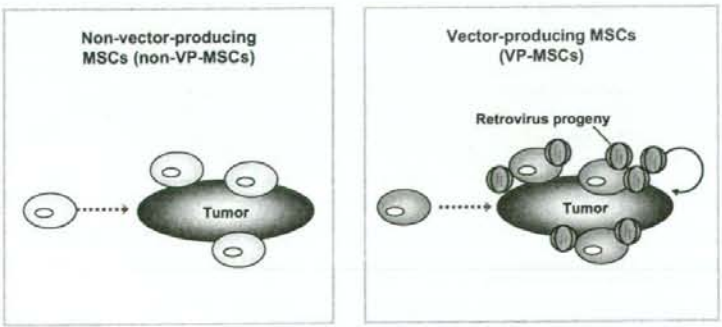

Fig. 3. Development of vector-producing tumor-tracking MSCs to augment suicide cancer gene therapy.

blasticidin S. Southern blot analysis of their genomic DNA revealed that three out of eight blasticidin S resistant clones showed site-specific integration of transgene into the AAVS1 site and that these clones had the GFP gene only at AAVS1. These results indicated that foreign DNA linked with ITR sequence could be targeted specifically into AAVS1 in KM-102 cells.

It is reported that the genome of myosin binding subunit 85 (MBS85) overlaps with the AAVS1 site [27]. To identify the junction between the transgene plasmid and the AAVS1 site, PCR was conducted using a transgene- and an AAVS1-specific primers. In two of the three clones the integration site was identified. In one clone the GFP gene was inserted at the first intron of MBS85 gene. The other clone had insertion of the GFP gene upstream of the first exon. Quantification of mRNA for MBS85 by real time PCR showed that the mRNA level decreased in these two KM-102 clones. The MBS85 is involved in the assembly of actin cytoskeleton. Although the outcome of allelic disruption of the MBS85 genome should be carefully evaluated, the system for AAVS1-specific integration of therapeutic DNA using AAV integration machinery is particularly valuable for *ex vivo* gene therapy applications for stem cells, such as ES cells and MSCs. For additional readings on the use of bone marrow cells for the treatment of autoimmunity, the reader is referred to companion papers published herein in this special issue of the Journal of Autoimmunity [28–38].

References

[1] Pittenger MF, Mackay AM, Beck SC, Jaiswal RK, Douglas R, Mosca JD, et al. Multilineage potential of adult human mesenchymal stem cells. Science 1999;284:143–7.

[2] Maitra B, Szekely E, Gjini K, Laughlin MJ, Dennis J, Haynesworth SE, et al. Human mesenchymal stem cells support unrelated donor hematopoietic stem cells and suppress T-cell activation. Bone Marrow Transplant 2004;33:597–604.

[3] Le Blanc K, Rasmusson I, Sundberg B, Götherström C, Hassan M, Uzunel M, et al. Treatment of severe acute graft-versus-host disease with third party haploidentical mesenchymal stem cells. Lancet 2004;363:1439–41.

[4] Ringden O, Uzunel M, Rasmusson I, Remberger M, Sundberg B, Lonnies H, et al. Mesenchymal stem cells for treatment of therapy-resistant graft-versus-host disease. Transplantation 2006;81:1390–7.

[5] Horwitz EM, Prockop DJ, Fitzpatrick LA, Koo WW, Gordon PL, Neel M, et al. Transplantability and therapeutic effects of bone marrow-derived mesenchymal cells in children with osteogenesis imperfecta. Nat Med 1999;5:309–13.

[6] Bang OY, Lee JS, Lee PH, Lee G. Autologous mesenchymal stem cell transplantation in stroke patients. Ann Neurol 2005;57:874–82.

[7] Nishikawa M, Ozawa K, Tojo A, Yoshikubo T, Okano A, Tani K, et al. Changes in hematopoiesis-supporting ability of C3H10T1/2 mouse embryo fibroblasts during differentiation. Blood 1993;81:1184–92.

[8] Oh I, Ozaki K, Miyazato A, Sato K, Meguro A, Muroi K, et al. Screening of genes responsible for differentiation of mouse mesenchymal stromal cells by DNA microarray analysis of C3H10T1/2 and C3H10T1/2-derived cell lines. Cytotherapy 2007;9:80–90.

[9] Sakamoto K, Yamaguchi S, Ando R, Miyawaki A, Kabasawa Y, Takagi M, et al. The nephroblastoma overexpressed gene (NOV/ccn3) protein associates with Notch1 extracellular domain and inhibits myoblast differentiation via Notch signaling pathway. J Biol Chem 2002;277:29399–405.

[10] Lijnen HR, Alessi MC, Van Hoef B, Collen D, Juhan-Vague I. On the role of plasminogen activator inhibitor-1 in adipose tissue development and insulin resistance in mice. J Thromb Haemost 2005;3:1174–9.

[11] Lassar AB, Buskin JN, Lockshon D, Davis RL, Apone S, Hauschka SD, et al. MyoD is a sequence-specific DNA binding protein requiring a region of myc homology to bind to the muscle creatine kinase enhancer. Cell 1989;58:823–31.

[12] Maekawa TL, Takahashi TA, Fujihara M, Urushibara N, Kadowaki-Kikuchi E, Nishikawa M, et al. A novel gene (drad-1) expressed in hematopoiesis-supporting stromal cell lines, ST2, PA6 and A54 preadipocytes: use of mRNA differential display. Stem Cells 1997;15:334–9.

[13] Mazini L, Wunder E, Sovalat H, Bourderont D, Baerenzung M, Bachorz J, et al. Mature accessory cells influence long-term growth of human hematopoietic progenitors on a murine stromal cell feeder layer. Stem Cells 1998;16:404–12.

[14] Arai F, Hirao A, Ohmura M, Sato H, Matsuoka S, Takubo K, et al. Tie2/angiopoietin-1 signaling regulates hematopoietic stem cell quiescence in the bone marrow niche. Cell 2004;118:149–61.

[15] Di Nicola M, Carlo-Stella C, Magni M, Milanesi M, Longoni PD, Matteucci P, et al. Human bone marrow stromal cells suppress T-lymphocyte proliferation induced by cellular or nonspecific mitogenic stimuli. Blood 2002;99:3838–43.

[16] Meisel R, Zibert A, Laryea M, Gobel U, Daubener W, Dilloo D. Human bone marrow stromal cells inhibit allogeneic T-cell responses by indoleamine 2,3-dioxygenase-mediated tryptophan degradation. Blood 2004;103:4619–21.

[17] Aggarwal S, Pittenger MF. Human mesenchymal stem cells modulate allogeneic immune cell responses. Blood 2005;105:1815–22.

[18] Albina JE, Abate JA, Henry Jr WL. Nitric oxide production is required for murine resident peritoneal macrophages to suppress mitogen-stimulated T cell proliferation: role of IFN-gamma in the induction of the nitric oxide-synthesizing pathway. J Immunol 1991;147:144–8.

[19] Sato K, Ozaki K, Oh I, Meguro A, Hatanaka K, Nagai T, et al. Nitric oxide plays a critical role in suppression of T cell proliferation by mesenchymal stem cells. Blood 2007;109:228–34.

[20] Oh I, Ozaki K, Sato K, Meguro A, Tatara R, Hatanaka K, et al. Interferon-gamma and NF-kappaB mediate nitric oxide production by mesenchymal stromal cells. Biochem Biophys Res Commun 2007;355:956–62.

[21] Studeny M, Marini FC, Dembinski JL, Zompetta C, Cabreira-Hansen M, Bekele BN, et al. Mesenchymal stem cells: potential precursors for tumor stroma and targeted-delivery vehicles for anticancer agents. J Natl Cancer Inst 2004;96:1593–603.

[22] Nakamizo A, Marini F, Amano T, Khan A, Studeny M, Gumin J, et al. Human bone marrow-derived mesenchymal stem cells in the treatment of gliomas. Cancer Res 2005;65:3307–18.

[23] Hall B, Dembinski J, Sasser AK, Studeny M, Andreeff M, Marini F. Mesenchymal stem cells in cancer: tumor-associated fibroblasts and cell-based delivery vehicles. Int J Hematol 2007;86:8–16.

[24] Surosky RT, Urabe M, Godwin SG, McQuinston SA, Kurtzman GJ, Ozawa K, et al. Adeno-associated virus Rep proteins target DNA sequences to a unique locus in the human genome. J Virol 1997;71:7951–9.

[25] Kogure K, Urabe M, Mizukami H, Kume A, Sato Y, Monahan J, et al. Targeted integration of foreign DNA into a defined locus on chromosome 19 in K562 cells using AAV-derived components. Int J Hematol 2001;73:469–75.

[26] Urabe M, Obara Y, Ito T, Mizukami H, Kume A, Ozawa K. Targeted insertion of transgene into a specific site on chromosome 19 by using adeno-associated virus integration machinery. In: Bertolotti R, Ozawa K, editors. Progress in gene therapy – vol. 3: autologous and cancer stem cell gene therapy. Singapore: World Scientific Publishing Co; 2007. p. 19–46.

[27] Dutheil N, Yoon-Robarts M, Ward P, Henckaerts E, Skrabanek L, Berns KI, et al. Characterization of the mouse adeno-associated virus AAVS1 ortholog. J Virol 2004;78:8917–21.

[28] Abraham N, Li M, Vanella L, Peterson S, Ikehara S, Asprinio D. Bone marrow stem cell transplant into intra-bone cavity prevent Type 2 diabetes: role of heme oxygenase and CO. J Autoimmunity 2008;30: 128–35.

[29] Boren E, Cheema G, Naguwa S, Ansari A, Gershwin M. The emergence of progressive multifocal leukoencephalopathy (PML) in rheumatic diseases. J Autoimmunity 2008;30:90–8.

[30] Burt R, Craig R, Cohen B, Suffit R, Barr W. Hematopoietic stem cell transplantation for autoimmune diseases: what have we learned? J Autoimmunity 2008;30:116–20.

[31] Deane S, Meyers F, Gershwin M. On reversing the persistence of memory: hematopoietic stem cell transplant for autoimmune disease in the first ten years. J Autoimmunity 2007;2008(30):180–96.

[32] Gershwin M. Bone marrow transplantation, refractory autoimmunity and the contributions of Susumu Ikehara. J Autoimmunity 2008;30: 105–7.

[33] Hara M, Murakami T, Kobayashi E. In vivo bioimaging using photogenic rats: fate of injected bone marrow-derived mesenchymal stromal cells. J Autoimmunity 2008;30:163–71.

[34] Ikehara S. A novel method of bone marrow transplantation (BMT) for intractable autoimmune diseases. J Autoimmunity 2008;30:108–15.

[35] Marmont A. Will hematopoietic stem cell transplantation cure human autoimmune diseases? J Autoimmunity 2008;30:145–50.

[36] Ratajczak M, Zuba-Surma E, Wysoczynski M, Wan W, Ratajczak J, Kucia M. Hunt for pluripotent stem cell – regenerative medicine search for almighty cell. J Autoimmunity 2008;30:151–62.

[37] Rezvani A, Storb R. Separation of graft-vs.-tumor effects from graft-vs.-host disease in allogeneic hematopoietic cell transplantation. J Autoimmunity 2008;30:172–9.

[38] Sonoda Y. Immunophenotype and functional characteristics of human primitive CD34-negative hematopoietic stem cells: the significance of the intra-bone marrow injection. J Autoimmunity 2008;30:136–44.

Oncogene (2009) 28, 231–242

www.nature.com/onc

ORIGINAL ARTICLE

Bortezomib overcomes cell adhesion-mediated drug resistance through downregulation of VLA-4 expression in multiple myeloma

K Noborio-Hatano[1,4], J Kikuchi[2,4], M Takatoku[1], R Shimizu[2], T Wada[2], M Ueda[1], M Nobuyoshi[1], I Oh[1], K Sato[1], T Suzuki[1], K Ozaki[1], M Mori[1], T Nagai[1], K Muroi[1], Y Kano[3], Y Furukawa[1,2] and K Ozawa[1]

[1]*Division of Hematology, Department of Internal Medicine, Jichi Medical University, Tochigi, Japan;* [2]*Division of Stem Cell Regulation, Center for Molecular Medicine, Jichi Medical University, Tochigi, Japan and* [3]*Division of Hematology, Department of Medical Oncology, Tochigi Cancer Center, Tochigi, Japan*

Multiple myeloma (MM) is incurable, mainly because of cell adhesion-mediated drug resistance (CAM-DR). In this study, we performed functional screening using short hairpin RNA (shRNA) to define the molecule(s) responsible for CAM-DR of MM. Using four *bona fide* myeloma cell lines (KHM-1B, KMS12-BM, RPMI8226 and U266) and primary myeloma cells, we identified CD29 (β1-integrin), CD44, CD49d (α4-integrin, a subunit of VLA-4), CD54 (intercellular adhesion molecule-1 (ICAM-1)), CD138 (syndecan-1) and CD184 (CXC chemokine receptor-4 (CXCR4)) as major adhesion molecules expressed on MM. shRNA-mediated knockdown of CD49d but not CD44, CD54, CD138 and CD184 significantly reversed CAM-DR of myeloma cells to bortezomib, vincristine, doxorubicin and dexamethasone. Experiments using blocking antibodies yielded almost identical results. Bortezomib was relatively resistant to CAM-DR because of its ability to specifically downregulate CD49d expression. This property was unique to bortezomib and was not observed in other anti-myeloma drugs. Pretreatment with bortezomib was able to ameliorate CAM-DR of myeloma cells to vincristine and dexamethasone. These results suggest that VLA-4 plays a critical role in CAM-DR of MM cells. The combination of bortezomib with conventional anti-myeloma drugs may be effective in overcoming CAM-DR of MM.
Oncogene (2009) **28,** 231–242; doi:10.1038/onc.2008.385; published online 13 October 2008

Keywords: myeloma; bortezomib; drug resistance; cell adhesion; VLA-4

Correspondence: Professor Y Furukawa, Division of Stem Cell Regulation, Center for Molecular Medicine, Jichi Medical University, 3311-1 Yakushiji, Shimotsuke, Tochigi 329-0498, Japan.
E-mail: furuyu@jichi.ac.jp
[4]These authors contributed equally to this work.
Received 2 June 2008; revised 19 August 2008; accepted 5 September 2008; published online 13 October 2008

Introduction

Despite recent advances in treatment strategies using dose-intensified regimens and new molecular-targeted compounds, multiple myeloma (MM) remains incurable (Kyle *et al.*, 2003). Most patients with MM eventually become resistant to the treatment and die of disease progression within 10 years. To improve the prognosis of myeloma patients, it is essential to overcome drug resistance (DR).

MM is characterized by the infiltration and growth of malignant plasma cells in the bone marrow (BM) microenvironment. MM cells localize within the BM through the interaction of adhesion receptors with their ligands on BM stromal cells and extracellular matrix proteins (Hideshima *et al.*, 2007). It has been demonstrated that MM cells in the BM microenvironment are much less sensitive to chemotherapeutic agents (Damiano *et al.*, 1999; Nefedova *et al.*, 2003). This type of DR has been termed cell adhesion-mediated DR (CAM-DR), which is believed to play a crucial role in both *de novo* and acquired DR in MM patients (Damiano *et al.*, 1999). Despite extensive investigations, the adhesion molecules critical for CAM-DR in MM have not been identified yet.

The proteasome inhibitor bortezomib (Velcade, formerly known as PS-341) has shown a clinical activity in patients with relapsed MM (Richardson *et al.*, 2003, 2005), and will be applied for the treatment of other hematologic malignancies and solid tumors in the near future (Fisher *et al.*, 2006; Davies *et al.*, 2007). Bortezomib is a reversible inhibitor of the 26S proteasome complex, which catalyses ubiquitin-dependent protein degradation. Inhibition of this complex ultimately leads to modulation of the abundance and functions of many intracellular proteins in bortezomib-treated cells (Hideshima *et al.*, 2001). Among them, the multifunctional transcription factor nuclear factor-kappa B (NF-κB) is considered the most relevant target in MM, because recent genome-wide approaches revealed that this factor is frequently activated in MM cells by mutations of the components of the NF-κB signaling cascade (Annunziata *et al.*, 2007; Keats *et al.*, 2007). Given the wide spectrum of transcriptional

targets of NF-κB including adhesion molecules and the IAP family of apoptosis inhibitors (Dolcet *et al.*, 2005), it is reasonable to speculate that CAM-DR of MM is mediated by NF-κB and could be overcome by bortezomib. To date, however, such possibilities have not been investigated.

In this study, we first attempted to identify the adhesion molecules responsible for CAM-DR in MM. By functional screening using the lentiviral short hairpin/small interfering RNA (shRNA/siRNA) system, we identified VLA-4 as a critical molecule for the induction of CAM-DR in MM cells. Furthermore, we found a novel and unique property of bortezomib to overcome CAM-DR by downregulating the expression of CD49d, a subunit of VLA-4. These results suggest that bortezomib enhances the effects of conventional anti-myeloma agents by overcoming VLA-4-mediated CAM-DR, and bortezomib-based combination chemotherapy can improve the treatment outcome of patients with MM.

Results

Surface expression of adhesion molecules on MM cells

In an initial effort to identify the molecules responsible for CAM-DR, we screened for the expression of adhesion molecules on MM cells using flow cytometry. By referring to previous studies (Tatsumi *et al.*, 1996; Cook *et al.*, 1997), we selected the molecules to be checked as follows: CD11a (lymphocyte function-associated antigen-1 (LFA-1)), CD18 (β2-integrin), CD22, CD29 (β1-integrin), CD40, CD44 (homing-associated cell adhesion molecule (HCAM)), CD49d (α4-integrin, a subunit of VLA-4), CD49e (α5-integrin, a subunit of VLA-5), CD54 (intercellular adhesion molecule-1 (ICAM-1)), CD56 (neural cell adhesion molecule (NCAM)), CD138 (syndecan-1) and CD184 (CXC chemokine receptor-4 (CXCR4)). We examined the expression of these molecules in four *bona fide* human MM cell lines (KHM-1B, KMS12-BM, RPMI8226 and U266) and normal plasma cells from healthy volunteers. As shown in Figure 1a, MM cell lines readily expressed CD29, CD44, CD49d, CD54, CD138 and CD184, whereas CD22 was barely detectable. The expression of CD11a, CD18, CD40, CD49e and CD56 was highly variable among cell lines. Normal plasma cells expressed the same set of molecules as MM cell lines except CD22, but their expression levels were generally lower than those of MM cells. It is of note that RPMI8226 showed a slightly different pattern from other cell lines: it expressed CD29, CD44 and CD49d lower but CD49e higher. Overall, we identified CD29, CD44, CD49d, CD54, CD138 and CD184 as major adhesion molecules expressed on MM cell lines.

To further elucidate the expression pattern of adhesion molecules in MM, we screened for their expression on primary MM cells. As CD138 is commonly used as a specific marker for myeloma cells in BM specimens, we detected the expression of CD44, CD49d and CD54 in CD138-positive fractions in BM-mononuclear cells (MNCs) from 18 patients with MM by dual staining on flow cytometry. As shown in Figure 1b, CD44, CD49d and CD54 were moderately to markedly expressed in all patients involved in this study. The proportions of positive cells were 52.8 ± 37.7% for CD44, 57.0 ± 31.6% for CD49d and 56.8 ± 30.9% for CD54 in the CD138-positive fractions (CD138 positivity was 60.0 ± 31.0% in the entire fraction). This pattern closely resembled that of the cell lines. On the basis of these results, we focused on CD29 (β1-integrin), CD44 (HCAM), CD49d (α4-integrin), CD54 (ICAM-1), CD138 (syndecan-1) and CD184 (CXCR4) to determine the functional adhesion molecules in MM in further studies.

Establishment of the in vitro *culture system for the assessment of CAM-DR of MM cells*

To investigate the involvement of these adhesion molecules in CAM-DR of MM cells, we established a culture system recapitulating CAM-DR *in vitro*. As described in Materials and methods, green fluorescent protein (GFP)-expressing MM cells were added into culture dishes with (co-culture) or without (stroma free) a preseeded UBE6T-7 stromal cell line, and cultured for 2 days in the absence or presence of four anti-myeloma drugs. We determined the cytotoxic effects of the drugs on MM cells specifically by measuring annexin-V positivity in GFP-positive fractions on flow cytometry. Figure 2a shows the representative results of KMS-12BM cells treated with suboptimal doses of each drug determined in pilot experiments: bortezomib 5 nM, vincristine 1 nM, doxorubicin 100 nM and dexamethasone 50 nM (Supplementary Figure S1). All of them are lower than clinically achievable concentrations *in vivo* according to recent clinical trials (Fisher *et al.*, 2006; Davies *et al.*, 2007). These drugs were capable of

Figure 1 Surface expression of adhesion molecules on multiple myeloma (MM) cells. (**a**) We screened for surface expression of adhesion molecules on MM cells using four myeloma cell lines (KHM-1B, KMS-12BM, RPMI8226 and U266) and normal plasma cells. Cells were stained with phycoerythrin (PE)-conjugated antibodies against CD11a (LFA-1), CD18 (β2-integrin), CD22, CD29 (β1-integrin), CD40, CD44 (HCAM), CD49d (α4-integrin), CD49e (α5-integrin), CD54 (ICAM-1), CD56 (NCAM), CD138 (syndecan-1), and CD184 (CXCR4), and subjected to flow cytometry. To analyse normal plasma cells, BM-MNCs were triple-stained with allophycocyanine (APC)-conjugated anti-CD38, PE-Cy7-conjugated anti-CD45 and PE-conjugated antibodies against each adhesion molecule. Cells in the $CD38^{+}/CD45^{lo/neg}$ fraction were gated as normal plasma cells. The means ± s.d. (bars) of three independent experiments are shown. (**b**) The expression of adhesion molecules was detected in primary MM cells. BM-MNCs were double-stained with an FITC-conjugated anti-CD138 antibody and PE-conjugated antibodies against CD44, CD49d and CD54. Each circle represents the positivity (%) of CD44, CD49d, and CD54 in the CD138-positive fractions, and that of CD138 in the entire fraction of BM-MNCs of individual patients (N = sample numbers). Bars indicate the average values of each molecule.

inducing apoptosis in more than 20% of KMS-12BM cells under stroma-free condition. In addition, we stained cells with propidium iodide to estimate the contribution of other forms of cell death to the cytotoxicity of these drugs. The percentages of dead cells obtained with propidium iodide staining were almost equal to or slightly higher than those obtained with annexin-V staining, implying that the major form

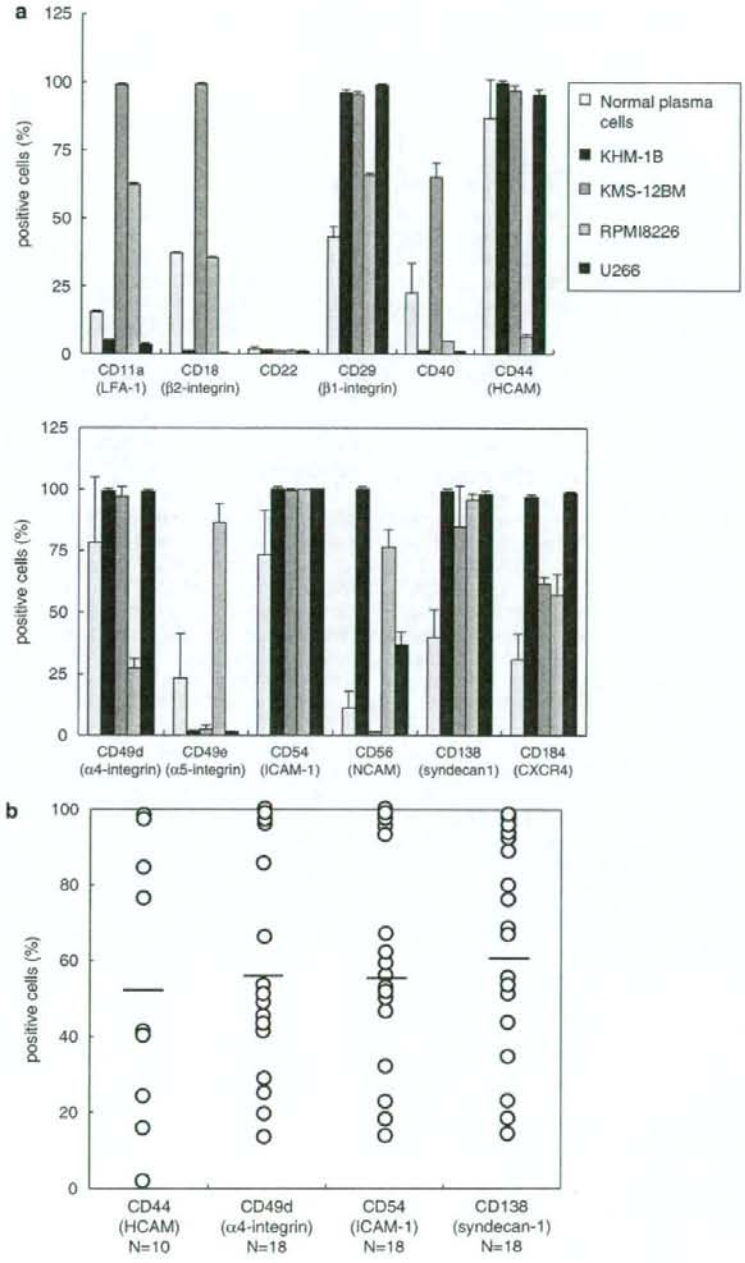

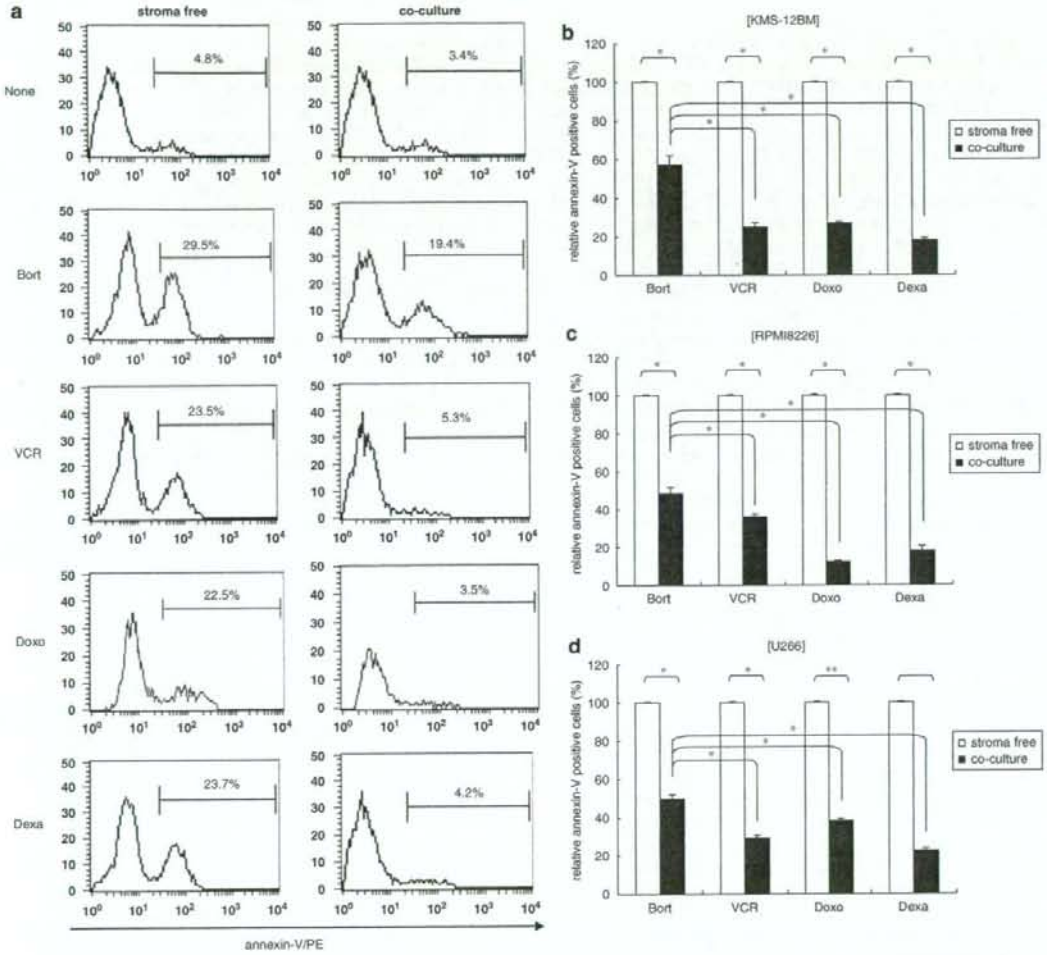

Figure 2 Establishment of the *in vitro* culture system for the assessment of cell adhesion-mediated drug resistance (CAM-DR) of multiple myeloma (MM) cells. (**a**) Green fluorescent protein (GFP)-transduced KMS-12BM cells were treated with either 5 nM bortezomib (Bort), 1 nM vincristine (VCR), 100 nM doxorubicin (Doxo) or 50 nM dexamethasone (Dexa) in the presence (co-culture) or absence (stroma free) of UBE6T-7 stromal cells for 48 h. Cell death/apoptosis was determined by reactivity with phycoerythrin (PE)-conjugated annexin-V (annexin-V/PE) in GFP-positive fractions on flow cytometry. Representative histogram plots are shown. Annexin-V positivity is indicated as a percentage in each histogram. (**b**) The *Y* axis shows the proportion of annexin-V-positive cells under co-culture condition with that under stroma-free condition setting at 100% in KMS-12BM cells treated with each drug. The means ± s.d. (bars) of three independent experiments are shown. The same experiments were carried out in RPMI8226 (**c**) and U266 (**d**). Drug concentrations were 2 nM for bortezomib, 1 nM for vincristine, 100 and 70 nM for doxorubicin, and 50 and 20 nM for dexamethasone in RPMI8226 and U266 cells, respectively. The *P*-values were calculated by Student's *t*-test. $^*P<0.05$.

of cell death is apoptosis (Supplementary Figure S2A). The cytotoxic effects were markedly diminished under the co-culture condition, suggesting that CAM-DR was successfully reproduced in our system (Figure 2a; Supplementary Figure S2). DR was not acquired in KMS-12BM cells cultured with stroma cells in trans-wells, which preclude direct cell-to-cell interactions, indicating that direct contact is indispensable for CAM-DR of MM (data not shown). As shown in Figures 2b–d and Supplementary Table S1, CAM-DR was similarly observed in all three myeloma cell lines treated with all four drugs tested, although the extent of CAM-DR was relatively low for bortezomib (discussed later). Furthermore, CAM-DR was reproduced with different concentrations of the drugs (Supplementary Figure S2b). Using this system, we attempted to

determine which adhesion molecule(s) is important for CAM-DR in MM cells.

Reversal of CAM-DR by shRNA/siRNA- and blocking antibody-mediated knockdown of VLA-4 in MM cells

To investigate which adhesion molecule(s) is critical for the acquisition of CAM-DR in MM cells, we performed loss-of-function analyses for CD44 (HCAM), CD49d (α4-integrin), CD54 (ICAM-1), CD138 (syndecan-1) and CD184 (CXCR4) using the shRNA/siRNA lentivirus system (Kikuchi *et al*., 2007). Because CD29 (β1-integrin) is heterodimerized with CD49d and functions as VLA-4 (α4β1-integrin) on MM cells, we could achieve loss of function of VLA-4 by solely targeting CD49d. As shown in Figure 3a, shRNA/siRNA expression vectors were constructed by inserting chemically synthesized oligonucleotides containing target sequences (Supplementary Table S2) into pLL3.7 vector, and their inhibitory activities were checked in KMS-12BM cells (data not shown). Constructs with the strongest activities were transfected into three MM cell lines along with sh controls, and a specific reduction of target expression was confirmed (Figure 3b; Supplementary Figure S3). Overall, we established 15 sublines in which the expression of individual adhesion molecules was markedly downregulated, and examined the levels of CAM-DR to four anti-myeloma drugs. To quantitatively assess the contribution of each molecule to CAM-DR, we defined the ratio of annexin-V reactivity of GFP-positive cells under the co-culture condition to that under the stroma-free condition as a reversal of CAM-DR. The reversal of CAM-DR to bortezomib was detectable in CD49d-knockdown sublines of all three cell lines, whereas no reversal was observed in sublines carrying shRNA/siRNA against other four adhesion molecules and inactive sh controls (Figure 3c; Supplementary Table S3). In addition, we performed the same experiments using vincristine and dexamethasone in KMS-12BM sublines. The CAM-DR to vincristine and dexamethasone was also reversed by knockdown of CD49d but not other four molecules (Figure 3d; Supplementary Table S4). It is of note that the reversal of CAM-DR to either vincristine or dexamethasone was at the almost equal level to that to bortezomib in CD49d-knockdown sublines (compare Figures 3c and d). In view of the fact that bortezomib is relatively resistant to CAM-DR (see Figure 2 and Supplementary Table S1), this implies that bortezomib modulates the expression of CD49d in MM cells (discussed later).

Furthermore, we confirmed the importance of CD49d in CAM-DR using adhesion-blocking antibodies instead of shRNA/siRNA introduction. We used specific antibodies against CD44, CD49d, CD54 and CD184 to revert CAM-DR, but were not able to test an anti-CD138 antibody because it is not commercially available. MM cells were pretreated with these antibodies, cultured with or without stromal cells in the presence of bortezomib, and subjected to flow cytometric analysis for annexin-V reactivity. As shown in Figure 4 and Supplementary Table S5, significant reversal of CAM-DR was achieved by treatment with anti-CD49d (α4-integrin) and anti-CD54 (ICAM-1) antibodies in KMS-12BM and U266 cells, albeit the effect of the former was much stronger. The effectiveness of anti-CD54 may stem from its effects on stromal cells, because previous studies revealed that CD54 was expressed on BM stromal cells (Corso *et al*., 2005). In contrast, the other antibodies failed to revert CAM-DR in KMS-12BM and U266 cells. Unexpectedly, CAM-DR was not affected by any antibodies in RPMI8226 cells, probably due to the relatively low expression of CD49d. Although there was slight discrepancy between the results obtained with shRNA/siRNA and adhesion-blocking antibodies, our data clearly indicate that VLA-4, a heterodimer of CD49d and CD29, is the most important adhesion molecule for CAM-DR in MM cells.

Downregulation of CD49d expression by bortezomib

It is tempting to speculate that bortezomib modulates the expression of CD49d in MM cells from our two findings: the relative resistance of bortezomib to CAM-DR (see Figure 2) and equal reversal of CAM-DR to all three drugs on disruption of VLA-4 signaling (see Figure 3). In support of this view, Duechler *et al*. (2005) reported that bortezomib decreased the surface expression of CD23 in chronic lymphocytic leukemia. Therefore, we investigated the effect of bortezomib and other anti-myeloma drugs on the expression of adhesion molecules on MM cell lines. Figure 5a and Supplementary Figure S4 show the representative data of flow cytometric analysis of viable KMS-12BM cells before and after treatment with bortezomib. Untreated KMS-12BM cells strongly expressed CD29, CD44, CD49d, CD54, CD138 and CD184. Bortezomib did not affect the expression levels of CD29, CD44, CD54, CD138 and CD184, but decreased the expression of CD49d from 99.4 ± 0.1 to $34.5 \pm 0.9\%$ ($n = 3$, $P < 0.05$). Bortezomib-induced downregulation of CD49d expression was similarly observed in RPMI8226 and U266 cells: from 33.2 ± 0.6 to $12.4 \pm 1.9\%$ in RPMI8226 cells ($n = 3$, $P < 0.05$) and from 99.4 ± 0.04 to $74.3 \pm 4.1\%$ in U266 cells ($n = 3$, $P < 0.05$). Furthermore, we confirmed bortezomib-mediated reduction of CD49d expression by immunoblotting using whole-cell lysates (Figure 5b), semiquantitative reverse transcription (RT)–PCR (Figure 5c) and real-time quantitative RT–PCR (Figure 5d), suggesting that this phenomenon takes place at mRNA levels. In striking contrast, other anti-myeloma drugs, such as vincristine, doxorubicin and dexamethasone, did not affect the expression of CD49d (Figure 5e; Supplementary Figure S4) and other adhesion molecules (Supplementary Figure S5) in any cell lines examined. The specific reduction of CD49d expression by bortezomib may underlie the relative resistance of the drug to CAM-DR in MM cells.

Next, we investigated the mechanisms by which bortezomib suppresses the expression of CD49d mRNA. For this purpose, we directly inhibited NF-κB activity in KMS-12BM cells using SN-50 peptide, which interferes with nuclear translocation of p50 by binding to its nuclear localization sequence (Lin *et al*., 1995). Surface expression of CD49d was not affected by the

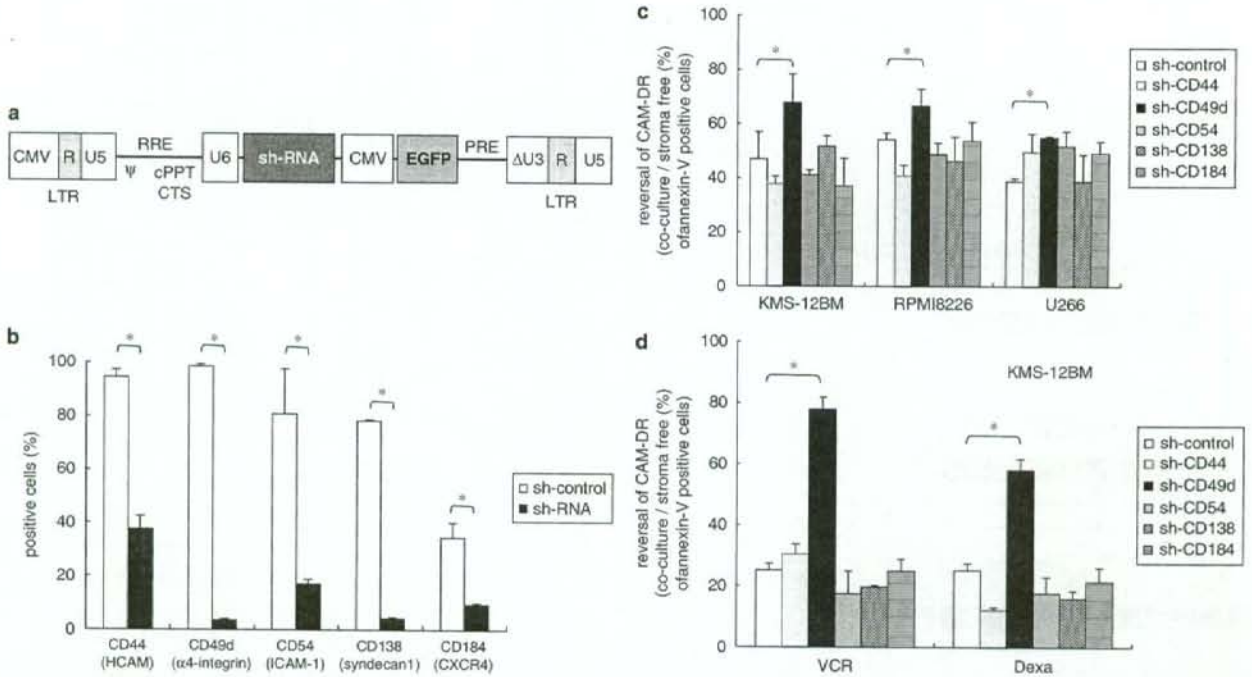

Figure 3 Effects of short hairpin RNA (shRNA)-mediated knockdown of adhesion molecules on adhesion-mediated drug resistance (CAM-DR) in multiple myeloma (MM) cells. (**a**) Schematic representation of a pLL3.7 lentiviral shRNA expression vector: U5 and U6 indicate U5 and U6 promoters, respectively; EGFP, enhanced green fluorescent protein; ψ, a packaging signal; RRE, rev-responsive element; cPPT, central polypurine tract; CTS, central termination sequence; CMV, cytomegalovirus promoter; PRE, wood-chuck hepatitis virus post-transcriptional regulatory element and LTR, long terminal repeat. See Materials and methods for details of construction. (**b**) KMS-12BM cells were transfected with either pLL3.7-sh-CD44, sh-CD49d, sh-CD54, sh-CD138, sh-CD184 or sh control vector. GFP-positive cells were collected by FACSaria flow cytometer, and stained with phycoerythrin (PE)-conjugated anti-CD44, anti-CD49d, anti-CD54, anti-CD138 and anti-CD184 antibodies, or PE-conjugated mouse and rat IgG isotype-matched controls. The means ± s.d. (bars) of three independent experiments are shown. The *P*-values were calculated by Student's *t*-test. $^*P<0.05$ against the sh control. (**c**) MM cell lines stably transfected with shRNA vectors were cultured with 2 nM bortezomib in the presence (co-culture) or absence (stroma free) of stromal cells. After 48 h, MM cells were harvested by pipetting, stained with annexin-V/PE, and subjected to flow cytometric analysis. The *Y* axis shows the reversal of CAM-DR as a ratio (%) of annexin-V positivity under co-culture vs stroma-free conditions. When annexin-V reactivity under co-culture condition is equal to that of stroma-free condition, the reversal of CAM-DR is 100%. The means ± s.d. (bars) of three independent experiments are shown. The *P*-values were calculated by Student's *t*-test. $^*P<0.05$ against the sh control. (**d**) KMS-12BM sublines stably transfected with shRNA vectors were cultured with 1 nM vincristine (VCR) or 50 nM dexamethasone (Dexa) in the presence (co-culture) or absence (stroma free) of stromal cells. After 48 h, the reversal of CAM-DR was examined as described above. $^*P<0.05$ against the sh control.

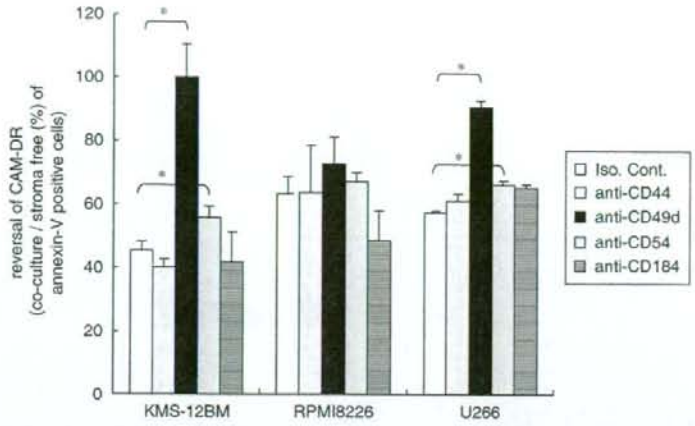

Figure 4 Effects of blocking antibodies against adhesion molecules on adhesion-mediated drug resistance (CAM-DR) in multiple myeloma (MM) cells. MM cell lines were treated with either antibodies against CD44, CD49d, CD54 and CD184 or isotype-matched controls (iso. cont.) at 10 μg/ml at 37 °C for 1 h. After treatment, cells were cultured with 2 nM bortezomib in the presence (co-culture) or absence (stroma free) of stromal cells for 48 h. The reversal of CAM-DR was determined as described in the legend of Figure 3. The means ± s.d. (bars) of three independent experiments are shown. The *P*-values were calculated by Student's *t*-test. $^*P<0.05$ against isotype-matched controls.

p50 inhibitory peptide, suggesting that bortezomib-mediated downregulation of CD49d is not a direct consequence of the inhibition of NF-κB activity (Supplementary Figure S6).

The reversal of CAM-DR to conventional anti-myeloma drugs by pretreatment with bortezomib

Given that bortezomib decreases the expression of CD49d, which plays a crucial role in CAM-DR, pretreatment of MM cells with bortezomib could overcome CAM-DR to conventional anti-myeloma drugs. Finally, we tested this hypothesis using the co-culture system for CAM-DR. MM cells were pretreated with bortezomib for 24 h, followed by exposure to either vincristine or dexamethasone for additional 24 h in the presence or absence of stroma cells. Pretreatment with bortezomib significantly reversed CAM-DR to both vincristine and dexamethasone in all three cell lines tested (Figure 6a), which coincided with the detachment of myeloma cells (Figure 6b). In particular, CAM-DR to VCR was almost completely inhibited in KMS-12BM and RPMI8226 cells: reversal ratios were 87.4 ± 3.2 and 104.6 ± 19.4%, respectively. In U266 cells, the effects of bortezomib were moderate but significant. This may be attributable to the relatively weak effects of bortezomib on CD49d expression in U266 cells (see Figure 5d). It should be emphasized that the combination of bortezomib with either vincristine or dexamethasone at the doses used in this experiment did not show additive effects under stroma-free condition (data not shown).

Discussion

In this study, we have clearly demonstrated that VLA-4, a heterodimer of CD49d/CD29, plays a critical role in CAM-DR of MM using a unique strategy involving myeloma cell lines in which individual adhesion molecules were stably knocked down by the aid of shRNA. In support of our finding, several studies described the roles of VLA-4 in the pathophysiology of MM. For example, CD29-mediated adhesion of MM cells to fibronectin upregulated the expression of the CDK inhibitor p27 and induced NF-κB activation, both of which confer CAM-DR to MM (Chauhan *et al.*, 1996; Hazlehurst *et al.*, 2000; Landowski *et al.*, 2003). Two independent groups reported that administration of anti-CD49d antibody suppressed the growth of MM cells in murine xenograft models (Mori *et al.*, 2004; Olson *et al.*, 2005). In line with these experimental findings, Schmidmaier *et al.* (2006) found that MM patients with primary multidrug resistance showed significantly higher concentrations of serum VLA-4 and ICAM-1 than responders. The involvement of VLA-4 in CAM-DR was also demonstrated in AML by the seminal study of Matsunaga *et al.* (2003), in which the combination of cytosine arabinoside and anti-CD49d antibody achieved a 100% survival rate in mice transplanted with AML cells. These findings strongly suggest that VLA-4-mediated signaling is important for the development of DR in MM and AML cells both *in vitro* and *in vivo*.

In addition, we obtained evidence indicating that bortezomib can overcome CAM-DR by selectively downregulating CD49d expression in myeloma cells. This ability was specific for bortezomib and was not observed in other commonly used anti-myeloma drugs such as vincristine, doxorubicin and dexamethasone. Moreover, we have found that bortezomib represses the expression of CD49d at mRNA levels. Regarding the mechanisms of this phenomenon, the direct involvement of NF-κB is unlikely because the p50 inhibitory peptide

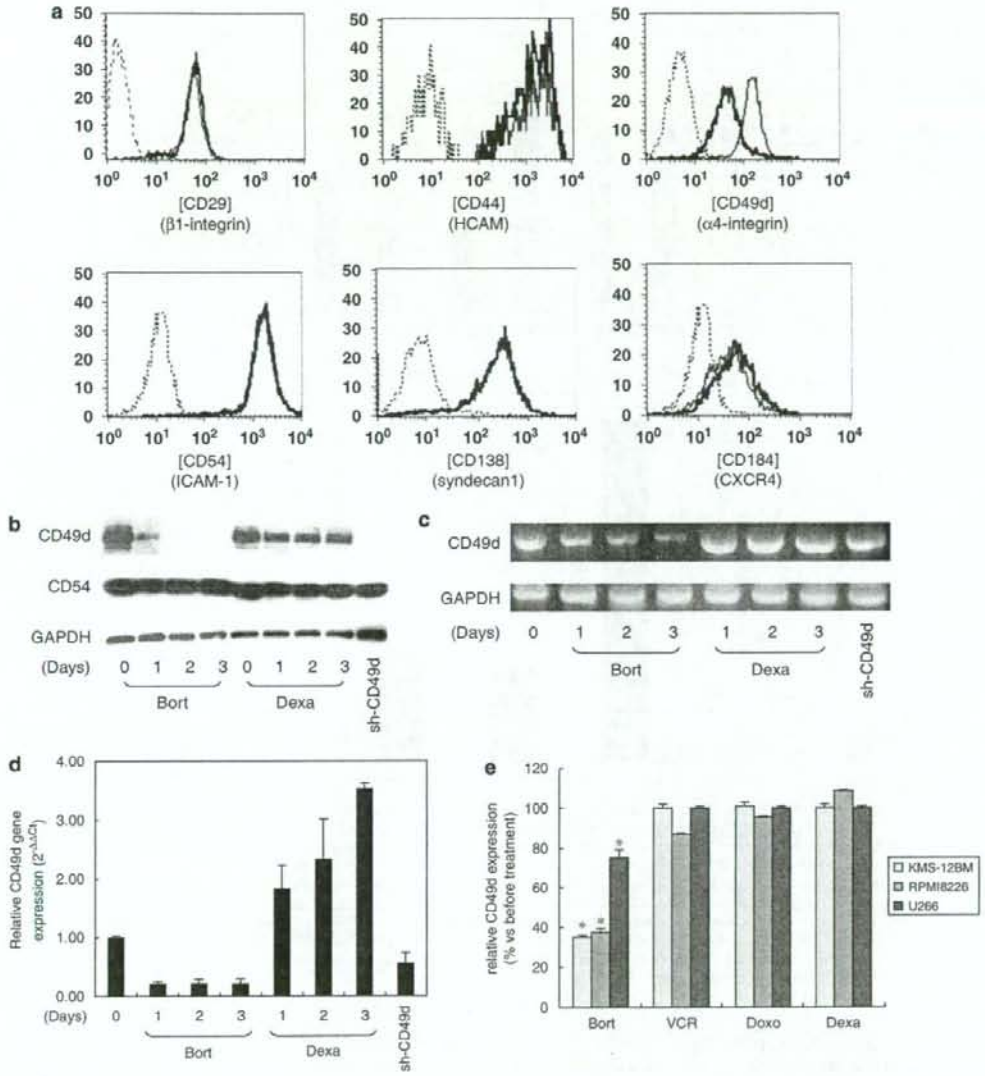

Figure 5 Effects of anti-myeloma drugs on the expression of adhesion molecules in multiple myeloma (MM) cells. (**a**) Surface expression of CD29, CD44, CD49d, CD54, CD138 and CD184 was detected by flow cytometry on KMS-12BM cells before and after treatment with 5 nM bortezomib for 48 h. Thin lines, bold lines and dotted lines show plots before treatment, after treatment and of isotype-matched controls, respectively. Representative histograms of three independent experiments are shown. (**b**) KMS12-BM cells were treated with either 5 nM bortezomib (Bort) or 50 nM dexamethasone (Dexa) for up to 3 days. We used a KMS12-BM subline transfected with pLL3.7-sh-CD49d (sh-CD49d) as a control. Cells were harvested at the indicated time points, and subjected to immunoblot analysis for the expression of CD49d, CD54 and GAPDH (loading control). (**c**) Total cellular RNA was isolated simultaneously at the experiments described in (**b**), and subjected to semiquantitative reverse transcription (RT)-PCR for the expression of CD49d and GAPDH (loading control). (**d**) Total cellular RNA was isolated simultaneously at the experiments described in (**b**), and subjected to real-time quantitative reverse transcription (RT)-PCR. The expression of CD49d was normalized to that of GAPDH and quantified by the $2^{-\Delta\Delta Ct}$ method. (**e**) The expression of CD49d was detected before and after bortezomib treatment in KMS-12BM, RPMI8226 and U266 MM cells by flow cytometry. The concentrations of bortezomib were 5, 2 and 2 nM for KMS-12BM, RPMI8226 and U266 cells, respectively. Data shown are the means ± s.d. (bars) of relative CD49d expression (ratio (%) of CD49d positivity after vs before treatment) of three independent experiments. The *P*-values were calculated by Student's *t*-test. $^{*}P<0.05$ against the values obtained before treatment.

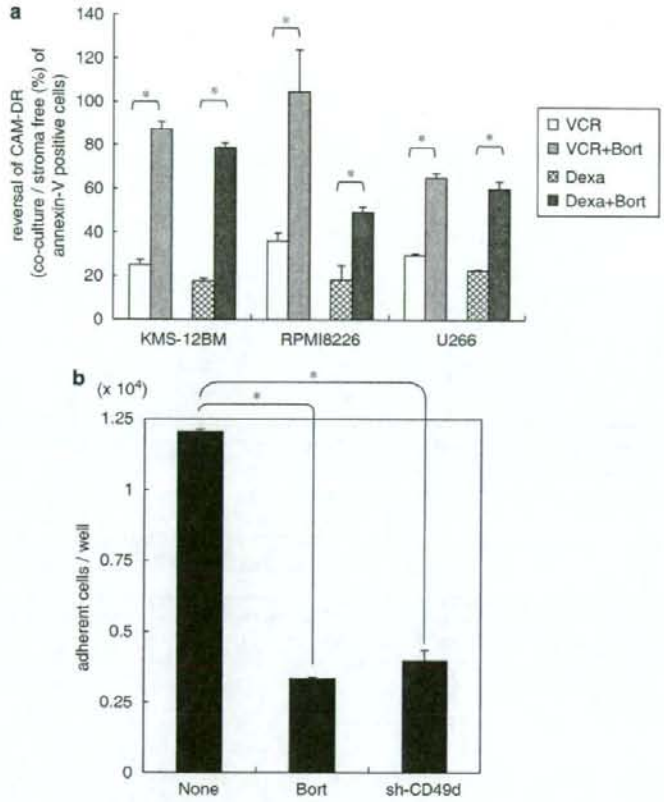

Figure 6 Bortezomib overcomes adhesion-mediated drug resistance (CAM-DR) to vincristine and dexamethasone in multiple myeloma (MM) cells. (**a**) Three myeloma cell lines were treated with 2 nM bortezomib for 24 h. After washing, we cultured cells with either vincristine (Bort + VCR) or dexamethasone (Bort + Dexa) in the absence or presence of stromal cells for additional 24 h. As controls, we carried out the same experiments without pretreatment of bortezomib (VCR and Dexa). The reversal of CAM-DR was determined as described in the legend of Figure 3. (**b**) Green fluorescent protein (GFP)-transduced KMS12-BM cells were cultured in the absence (None) or presence (Bort) of 5 nM bortezomib for 3 days. We used a KMS12-BM subline transfected with pLL3.7-sh-CD49d (sh-CD49d) as a control. Cells were then co-cultured with UBE6T-7 cells at 37 °C for 15 min. Non-adherent cells were washed off with phosphate-buffered saline (PBS), and resultant adherent cells were harvested with trypsin-EDTA. We determined GFP positivity (%) in non-adherent cells using flow cytometer. The means ± s.d. (bars) of three independent experiments are shown. The *P*-values were calculated by Student's *t*-test (*$P<0.05$).

did not downregulate the expression of CD49d in KMS-12BM cells, in which NF-κB is constitutively activated through the classical pathway (Keats *et al.*, 2007). The CD49d promoter contains canonical binding sites for Sp1, Ets and WT1 (Rosen *et al.*, 1994; Zutter *et al.*, 1997; Kirschner *et al.*, 2006). We are currently investigating whether these factors are implicated in bortezomib-mediated downregulation of CD49d mRNA expression.

The reversal of CAM-DR by bortezomib may underlie its broad range of synergy with other anticancer drugs as recently described (Horton *et al.*, 2006; Noborio-Hatano *et al.*, 2007). Unfortunately, severe pulmonary complications have been reported in Japanese patients treated with bortezomib (Miyakoshi *et al.*, 2006). Dose reduction by drug combination is one method to minimize side effects of bortezomib. Furthermore, it has been shown that the contact of MM cells with BM stromal cells through VLA-4/vascular cell adhesion molecule-1 (VCAM-1) interactions enhanced the production of osteoclastogenesis factors and that disruption of this cell-to-cell contact suppressed the development of osteoclastic osteolysis associated with MM (Michigami *et al.*, 2000; Pearse *et al.*, 2001). As bortezomib can suppress CD49d expression, this drug may also be effective for the amelioration of bone lesions in MM.

Although our findings provide rationale for safe and effective treatment strategies for refractory myeloma, further investigation is required to define suitable combinations involving not only conventional anti-myeloma drugs but also new drugs such as lenalidomide.

Previous studies revealed that both bortezomib and dexamethasone induced apoptosis primarily through caspase-9, whereas lenalidomide did so through caspase-8 (Mitsiades *et al.*, 2002). Indeed, we found that caspase-8 was not activated in MM cells by the drugs used in this study (data not shown). On the basis of these findings, the combination of lenalidomide with either bortezomib or dexamethasone is expected to trigger dual apoptotic signaling pathways and reverse DR, which results in the achievement of clinical responses in patients resistant to single agents. In support of this view, we have reported that bortezomib is effective for myeloma patients refractory to thalidomide therapy (Takatoku *et al.*, 2004). The combination of bortezomib with other anti-myeloma drugs, including thalidomide and its derivatives, is effective for overcoming CAM-DR and may improve the prognosis of MM patients.

Materials and methods

Cells and cell culture

We used four *bone fide* human MM cell lines, KHM-1B, KMS-12BM, RPMI8226 and U266, in this study (Drexler *et al.*, 2003). These cell lines were purchased from the Health Science Research Resources Bank (Osaka, Japan), and maintained in RPMI1640 medium (Sigma Co., St Louis, MO, USA) supplemented with 10% heat-inactivated fetal calf serum (Sigma Co.,) and antibiotics. Human BM-derived stromal cell line UBE6T-7 (Mori *et al.*, 2005), which was transduced with a human telomerase catalytic protein subunit, was kindly provided by Dr Akihiro Umezawa (National Research Institute for Child Health and Development, Tokyo, Japan), and used as stromal cells in co-culture experiments. Primary MM cells were isolated from the BM of patients at the time of diagnostic procedure. CD38-positive/CD45-low or negative ($CD38^+/CD45^{lo/neg}$) cells were purified from the BM of healthy volunteers, and used as normal plasma cells. Informed consent was obtained in accordance with the Declaration of Helsinki, and the protocol was approved by the Institutional Review Board.

Drugs and adhesion-blocking antibodies

Bortezomib (Velcade) was provided by Millennium Pharmaceuticals (Cambridge, MA, USA). We used vincristine (Shionogi Co. Ltd., Tokyo, Japan), doxorubicin (Meiji Co. Ltd., Tokyo, Japan) and dexamethasone (Sigma Co.) as conventional anti-myeloma drugs. All drugs were dissolved in RPMI1640 medium at appropriate concentrations and stored at −80 °C until use. We used the following adhesion-blocking antibodies in co-culture experiments: anti-CD44 (clone Hermes-1; Endogen, Rockford, IL, USA), anti-CD49d (2B4; R&D Systems, Minneapolis, MN, USA), anti-CD54 (Ab-2; Labvision Corp., Fremont, CA, USA), anti-CD184 (44717.111; R&D Systems), and mouse or rat IgG isotype controls (eBioscience, San Diego, CA, USA). Blocking experiments were performed as described earlier. In brief, 1×10^6 of MM cells were incubated with 10 μg/ml antibodies or isotype-matched controls in 100 μl of RPMI1640 medium for 1 h, then diluted to 2×10^5 cells/ml in complete medium, and added into culture wells preseeded with stromal cells (Matsunaga *et al.*, 2003).

Flow cytometric analysis of adhesion molecules

Cells were stained with specific monoclonal antibodies and analysed using BD-LSR or FACSaria flow cytometer (Becton Dickinson, Oxford, UK) as described earlier (Kikuchi *et al.*, 2005). The antibodies used were phycoerythrin (PE)-conjugated antibodies against CD11a (clone HI 111; BioLegend, San Diego, CA, USA), CD29 (4B4; Beckman Coulter, Fullerton, CA, USA), CD18 (6.7), CD22 (HIB22), CD29 (HUTS-21), CD49e (IIA1), CD56 (B159), CD138 (MI15) and CD184 (12G5) (all from Becton Dickinson), CD40 (5C3), CD44 (G44-26), CD49d (9F10) and CD54 (HA58) (all from eBioscience), allophycocyanine-conjugated antibodies against CD38 (HB7; Becton Dickinson) and PE-Cy7-conjugated antibodies against CD45 (2D1; Becton Dickinson).

Cell proliferation assay

Cell proliferation was monitored using Cell Counting Kit-8 (Dojin Chemical, Tokyo, Japan). In brief, cells were seeded in 96-well flat-bottomed microplates at a density of 5×10^4 per well and incubated with or without anti-myeloma drugs for 48 h at 37 °C. After incubation, 10 μl of WST-8 solution was added to each well at a final concentration of 1 μg/ml. Cells grown in complete medium alone were used as controls. After incubation at 37 °C for 4 h, absorbance was measured at a wavelength of 450 nm using a microplate reader.

Co-culture of MM cells with stromal cells and the assessment of cell death

For co-culture experiments, we established GFP-expressing MM cell lines by transfecting GFP expression plasmids to distinguish MM cells from stromal cells. UBE6T-7 stromal cells were seeded in 48-well plates to near confluence. After stromal cells were washed once with fresh medium, GFP-transduced MM cells were added to the plates and cultured in the absence or presence of anti-myeloma drugs. After 48 h, the cells were harvested by pipetting, washed with phosphate-buffered saline, and stained with PE-conjugated annexin-V (annexin-V/PE) (Biovision, Mountain View, CA, USA). Cell death/apoptosis was judged by annexin-V reactivity in GFP-positive populations using flow cytometer (Yanamandra *et al.*, 2006).

Construction and production of lentiviral shRNA/siRNA expression vectors

We used a lentiviral shRNA/siRNA expression vector pLL3.7. for knockdown of adhesion molecules. siRNA target sequences were designed to be homologous to wild-type cDNA sequences. Oligonucleotides were chemically synthesized, annealed, terminally phosphorylated and inserted into pLL3.7 vector. Oligonucleotides containing siRNA target sequences were shown in Supplementary Table S1. Ineffective sequences were used as sh controls. These vectors were co-transfected into 293FT cells with packaging plasmids (purchased from Invitrogen, Carlsbad, CA, USA). Infectious lentiviruses in culture supernatants were harvested, concentrated and infected as described earlier (Kikuchi *et al.*, 2007). Lentiviruses were then added into cell suspensions in the presence of 8 μg/ml polybrene, and transduced for 24 h. Transduction efficiencies were monitored by GFP expression using a flow cytometer.

Immunoblotting

Immunoblotting was carried out according to the standard method using the following antibodies: anti-CD49d (Novus Biologicals, Littleton, CO, USA), anti-CD54 (Santa Cruz Biotechnology, Santa Cruz, CA, USA), anti-caspase-8, anti-caspase-9 (Becton Dickinson) and anti-GAPDH (Santa Cruz Biotechnology) (Odgerel *et al.*, 2008).

PCR

We performed semiquantitative RT–PCR and real-time quantitative RT–PCR to estimate the expression of CD49d at mRNA levels. For the former, PCR amplification was carried out with 1 μl of cDNA solution (corresponding to 50 ng total RNA) in a 50-μl reaction mixture containing 5 U of *Taq* polymerase, 10 mM Tris-HCl (pH 8.5), 50 mM KCl, 1.5 mM $MgCl_2$ and 100 mM dNTPs in the presence of specific primer pairs (200 nM each) as follows; CD49d, forward: 5′-GGATGT GAACAGAAAGGCAGA-3′, reverse: 5′-GCCAGTGTTGA TAACATGGAAA-3′; GAPDH (internal control), forward: 5′-CCACCCATGGCAAATTCCATGGCA-3′, reverse: 5′-TCTAGACGGCAGGTCAGGTCCACC-3′. PCR products were resolved on 2% agarose gels, and visualized by staining with ethidium bromide. The results of 40 amplification cycles are shown. For the latter, we used the same primer pairs in the SYBR Green PCR system (Applied Biosystems, Foster City, CA, USA). Data quantification was carried out by the $2^{-\Delta\Delta C_t}$ method (Pfaffl, 2001).

Acknowledgements

This study was supported in part by grants from the Ministry of Health, Welfare, and Labor of Japan, and Grants-in-Aid for Scientific Research from the Ministry of Education, Science, Sports, and Technology of Japan. KN-H and JK are winners of the Jichi Medical School Young Investigator Award.

References

Annunziata CM, Davis RE, Demchenko Y, Bellamy W, Gabrea A, Zhan F *et al.* (2007). Frequent engagement of the classical and alternative NF-κB pathways by diverse genetic abnormalities in multiple myeloma. *Cancer Cell* **12**: 115–130.

Chauhan D, Uchiyama H, Akbarali Y, Urashima M, Yamamoto K, Libermann TA *et al.* (1996). Multiple myeloma cell adhesion-induced interleukin-6 expression in bone marrow stromal cells involves activation of NF-κB. *Blood* **87**: 1104–1112.

Cook G, Dumbar M, Franklin IM. (1997). The role of adhesion molecules in multiple myeloma. *Acta Haematol* **97**: 81–89.

Corso A, Ferretti E, Lunghi M, Zappasodi P, Mangiacavalli S, De Amici M *et al.* (2005). Zoledronic acid down-regulates adhesion molecules of bone marrow stromal cells in multiple myeloma: a possible mechanism for its antitumor effect. *Cancer* **104**: 118–125.

Damiano JS, Cress AE, Hazlehurst LA, Shtil AA, Dalton WS. (1999). Cell adhesion mediated drug resistance (CAM-DR): role of integrins and resistance to apoptosis in human myeloma cell lines. *Blood* **93**: 1658–1667.

Davies AM, Lara Jr PN, Mack PC, Gandara DR. (2007). Incorporating bortezomib into the treatment of lung cancer. *Clin Cancer Res* **13**: 4647s–4651s.

Dolcet X, Llobet D, Pallares J. (2005). NF-κB in development and progression of human cancer. *Virchows Arch* **446**: 475–482.

Drexler HG, Matsuo Y, MacLeod RA. (2003). Persistent use of false myeloma cell lines. *Hum Cell* **16**: 101–105.

Duechler M, Shehata M, Schwarzmeier JD, Hoelbl A, Hilgarth M, Hubmann R. (2005). Induction of apoptosis by proteasome inhibitors in B-CLL cells is associated with downregulation of CD23 and inactivation of Notch2. *Leukemia* **19**: 260–267.

Fisher RI, Bernstein SH, Kahl BS, Djulbegovic B, Robertson MJ, de Vos S *et al.* (2006). Multicenter phase II study of bortezomib in patients with relapsed or refractory mantle cell lymphoma. *J Clin Oncol* **24**: 4867–4874.

Hazlehurst LA, Damiano JS, Buyuksal I, Pledger WJ, Dalton WS. (2000). Adhesion to fibronectin via β1 integrins regulates $p27^{kip1}$ levels and contributes to cell adhesion mediated drug resistance (CAM-DR). *Oncogene* **19**: 4319–4327.

Hideshima T, Mitsiades C, Tonon G, Richardson PG, Anderson KC. (2007). Understanding multiple myeloma pathogenesis in the bone marrow to identify new therapeutic targets. *Nat Rev Cancer* **7**: 585–598.

Hideshima T, Richardson P, Chauhan D, Palombella VJ, Elliott PJ, Adams J *et al.* (2001). The proteasome inhibitor PS-341 inhibits growth, induces apoptosis, and overcomes drug resistance in human multiple myeloma cells. *Cancer Res* **61**: 3071–3076.

Horton TM, Gannavarapu A, Blaney SM, D'Argenio DZ, Plon SE, Berg SL. (2006). Bortezomib interactions with chemotherapy agents in acute leukemia *in vitro*. *Cancer Chemother Pharmacol* **58**: 13–23.

Keats JJ, Fonseca R, Chesi M, Schop R, Baker A, Chng WJ *et al.* (2007). Promiscuous mutations activate the noncanonical NF-κB pathway in multiple myeloma. *Cancer Cell* **12**: 131–144.

Kikuchi J, Ozaki H, Nonomura C, Shinohara H, Iguchi S, Nojiri H *et al.* (2005). Transfection of antisense core 2 β1,6-*N*-acetylglucosaminyltransferase-1 cDNA suppresses selectin ligand expression and tissue infiltration of B-cell precursor leukemia cells. *Leukemia* **19**: 1934–1940.

Kikuchi J, Shimizu R, Wada T, Ando H, Nakamura M, Ozawa K *et al.* (2007). E2F-6 suppresses growth-associated apoptosis of human hematopoietic progenitor cells by counteracting proapoptotic activity of E2F-1. *Stem Cells* **25**: 2439–2447.

Kirschner KM, Wagner N, Wagner KD, Wellmann S, Scholz H. (2006). The Wilms tumor suppressor Wt1 promotes cell adhesion through transcriptional activation of the α4 integrin gene. *J Biol Chem* **281**: 31930–31939.

Kyle RA, Gertz MA, Witzig TE, Lust JA, Lacy MQ, Dispenzieri A *et al.* (2003). Review of 1027 patients with newly diagnosed multiple myeloma. *Mayo Clin Proc* **78**: 21–33.

Landowski TH, Olashaw NE, Agrawal D, Dalton WS. (2003). Cell adhesion-mediated drug resistance (CAM-DR) is associated with activation of NF-κB (RelB/p50) in myeloma cells. *Oncogene* **22**: 2417–2421.

Lin YZ, Yao SY, Veach RA, Torgerson TR, Hawiger J. (1995). Inhibition of nuclear translocation of transcription factor NF-κB by a synthetic peptide containing a cell membrane-permeable motif and nuclear localization sequence. *J Biol Chem* **270**: 14255–14258.

Matsunaga T, Takemoto N, Sato T, Takimoto R, Tanaka I, Fujimi A *et al.* (2003). Interaction between leukemic-cell VLA-4 and stromal fibronectin is a decisive factor for minimal residual disease of acute myelogenous leukemia. *Nat Med* **9**: 1158–1165.

Michigami T, Shimizu N, Williams PJ, Niewolna M, Dallas SL, Mundy GR *et al.* (2000). Cell–cell contact between marrow stromal cells and myeloma cells via VCAM-1 and α4β1-integrin enhances production of osteoclast-stimulating activity. *Blood* **96**: 1953–1960.

Mitsiades N, Mitsiades CS, Poulaki V, Chauhan D, Richardson PG, Hideshima T *et al.* (2002). Apoptotic signaling induced by immunomodulatory thalidomide analogs in human multiple myeloma cells: therapeutic implications. *Blood* **99**: 4525–4530.

Miyakoshi S, Kami M, Yuji K, Matsumura T, Takatoku M, Sasaki M *et al.* (2006). Severe pulmonary complications in Japanese patients after bortezomib treatment for refractory multiple myeloma. *Blood* **107**: 3492–3494.

Mori T, Kiyono T, Imabayashi H, Takeda Y, Tsuchiya K, Miyoshi S *et al.* (2005). Combination of hTERT and bmi-1, E6, or E7 induces prolongation of the life span of bone marrow stromal cells from an elderly donor without affecting their neurogenic potential. *Mol Cell Biol* **25**: 5183–5195.

Mori Y, Shimizu N, Dallas M, Niewolna M, Story B, Williams PJ *et al.* (2004). Anti-α4 integrin antibody suppresses the development of multiple myeloma and associated osteoclastic osteolysis. *Blood* **104**: 2149–2154.

Nefedova Y, Landowski TH, Dalton WS. (2003). Bone marrow stromal-derived soluble factors and direct cell contact contribute to

de novo drug resistance of myeloma cells by distinct mechanisms. *Leukemia* **17**: 1175–1182.

Noborio-Hatano K, Kano Y, Akustu M, Kikuchi J, Ueda M, Takatoku M *et al.* (2007). Effects of bortezomib in combination with conventional drugs against human lymphoid cell lines. *Jpn J Clin Hematol* **48**: 1093a.

Odgerel T, Kikuchi J, Wada T, Shimizu R, Futaki K, Kano Y *et al.* (2008). The FLT3 inhibitor PKC412 exerts differential cell cycle effects on leukemic cells depending on the presence of FLT3 mutations. *Oncogene* **27**: 3102–3110.

Olson DL, Burkly LC, Leone DR, Dolinski BM, Lobb RR. (2005). Anti-α4 integrin monoclonal antibody inhibits multiple myeloma growth in a murine model. *Mol Cancer Ther* **4**: 91–99.

Pearse RN, Sordillo EM, Yaccoby S, Wong BR, Liau DF, Colman N *et al.* (2001). Multiple myeloma disrupts the TRANCE/osteoprotegerin cytokine axis to trigger bone destruction and promote tumor progression. *Proc Natl Acad Sci USA* **98**: 11581–11586.

Pfaffl MW. (2001). A new mathematical model for relative quantification in real-time RT–PCR. *Nucleic Acid Res* **29**: e45.

Richardson PG, Barlogie B, Berenson J, Singhal S, Jagannath S, Irwin D *et al.* (2003). A phase 2 study of bortezomib in relapsed, refractory myeloma. *N Engl J Med* **348**: 2609–2617.

Richardson PG, Sonneveld P, Schuster MW, Irwin D, Stadtmauer EA, Facon T *et al.* (2005). Assessment of proteasome inhibition for extending remissions (APEX) investigators. Bortezomib or high-dose dexamethasone for relapsed multiple myeloma. *N Engl J Med* **352**: 2487–2498.

Rosen GD, Barks JL, Iademarco MF, Fisher RJ, Dean DC. (1994). An intricate arrangement of binding sites for the Ets family of transcription factors regulates activity of the α4 integrin gene promoter. *J Biol Chem* **269**: 15652–15660.

Schmidmaier R, Morsdorf K, Baumann P, Emmerich B, Meinhardt G. (2006). Evidence for cell adhesion-mediated drug resistance of multiple myeloma cells *in vivo*. *Int J Biol Markers* **21**: 218–222.

Takatoku M, Noborio-Hatano K, Takahashi S, Kikuchi S, Mori M, Muroi K *et al.* (2004). Treatment with a proteasome inhibitor, bortezomib, for thalidomide-resistant multiple myeloma. *Jpn J Clin Hematol* **45**: 144–148.

Tatsumi T, Shimazaki C, Goto H, Araki S, Sudo Y, Yamagata N *et al.* (1996). Expression of adhesion molecules on myeloma cells. *Jpn J Cancer Res* **87**: 837–842.

Yanamandra N, Colaco NM, Parquet NA, Buzzeo RW, Boulware D, Wright G *et al.* (2006). Tipifarnib and bortezomib are synergistic and overcome cell adhesion-mediated drug resistance in multiple myeloma and acute myeloid leukemia. *Clin Cancer Res* **12**: 591–599.

Zutter MM, Ryan EE, Painter AD. (1997). Binding of phosphorylated Sp1 protein to tandem Sp1 binding sites regulates α2 integrin gene core promoter activity. *Blood* **90**: 678–689.

Supplementary Information accompanies the paper on the Oncogene website (http://www.nature.com/onc)

Leukemia & Lymphoma, February 2009; 50(2): 290–293

informa
healthcare

LETTER TO THE EDITOR

Prediction of response to imatinib in patients with chronic myelogenous leukemia by flow cytometric analysis of bone marrow blastic cell phenotypes

SATOKO OKA, KAZUO MUROI, MASAKI MORI, TOMOHIRO MATSUYAMA, SHIN-ICHIRO FUJIWARA, IEKUNI OH, KAZUYA SATO, SATORU KIKUCHI, MASUZU UEDA, MASAKI TOSHIMA, TAKAHIRO SUZUKI, KATSUTOSHI OZAKI, TADASHI NAGAI, & KEIYA OZAWA

Division of Hematology, Department of Medicine, Jichi Medical University Hospital, Shimotsuke, Tochigi, Japan

(Received 6 September 2008; revised 3 November 2008; accepted 15 November 2008)

Chronic myelogeneous leukemia (CML) is characterised by a specific translocation t(9; 22)(q34; q11), the Philadelphia (Ph) chromosome, giving rise to the novel BCR/ABL fusion gene [1]. The deregulated tyrosine kinase activity of the protein encoded by the fusion gene has been shown to be both necessary and sufficient for the initiation and maintenance of CML [1]. High response rates and favourable toxicities of imatinib in patients with newly diagnosed CML in chronic phase have been reported [2]. Imatinib induces a complete cytogenetic response (CCyR), i.e. disappearance of the Ph chromosome, in most patients with CML in chronic phase after one year of treatment with the drug [3–5]. However, some patients with CML in chronic phase who received treatment with imatinib show residual Ph chromosome after one year of treatment, and event-free survival in such patients was worse than that in patients showing a CCyR [3–5]. We analysed phenotypes of the cells in the blast region of bone marrow in CML by flow cytometry (FCM) and determined whether the phenotypes of the cells predict response to imatinib.

During the period from January 2005 to April 2007, 32 patients in Jichi University Hospital were diagnosed as having CML in chronic phase. The diagnosis of CML in chronic phase was based on peripheral blood pictures, bone marrow pictures and existence of the Ph chromosome in bone marrow. Three-colour FCM combined with two-colour FCM was performed to evaluate phenotypes of the cells in the blast region of bone marrow before the beginning of imatinib therapy. Bone marrow mononuclear cells were stained with fluorescein isothiocyanate-conjugated monoclonal antibody and/or phycoerythrin-conjugated monoclonal antibody and peridinin chlorophyll protein-conjugated CD45 [6,7]. Monoclonal antibodies used in this study were as follows: CD5, CD7, CD2, CD19, CD20, CD10, CD13, CD14, CD15, CD33, CD34, CD117, CD41, CD11b, CD11c, CD36, CD25, CD56, CD45 and HLA-DR. A gate was set for identifying immature cells characterised by intermediate CD45 expression and low side scatter properties [6,7]. Phenotypes of the cells in the blast region were analysed using a flow cytometer (FACSCalibur; BD Biosciences, San Jose, CA). Karyotypic analysis of bone marrow cells was performed using a standard Giemsa-banding method, and approximately 20 metaphases were analysed. BCR-ABL transcripts in bone marrow cells were measured using a real-time quantitative polymerase chain reaction assay (SRL Inc., Tokyo) [8]. All patients received treatment with imatinib only after the diagnosis of CML in chronic phase. To compare phenotypes of the cells in the blast region of bone marrow, bone marrow cells from patients with

Correspondence: Kazuo Muroi, MD, Jichi Medical University Hospital, Division of Hematology, Department of Medicine, 3311-1 Yakushii, Shimotsuke, Tochigi 329-0498, Japan. Tel: +81-285-58-7187. Fax: +81-285-44-5087. E-mail: muroi-kzu@jichi.ac.jp

ISSN 1042-8194 print/ISSN 1029-2403 online
DOI: 10.1080/10428190802627598

refractory anemia of myelodysplastic syndrome (MDS) and healthy volunteers were analysed by FCM as described earlier. *P* values below 0.05 were considered significant in the Mann–Whitney *U* test.

As shown in Table I, patients were divided into two groups according to the response after one year of treatment with imtinib: one group showing a CCyR (Group A) and other group not showing a CCyR (Group B). Group B was composed of five patients with minimal cytogenetic response and one patient with response failure [4]. There were no differences between the two groups in peripheral blood cell counts, peripheral blood blast percentages, peripheral blood basophil percentages, bone marrow blast percentages, bone marrow differentials and size of splenomegaly. Additional chromosomal abnormalities were detected in one patient of Group A. There was a tendency for older age in patients of Group A. The mean dose of imatinib per day was higher in Group A than in Group B, but the difference was not significant. There were differences between the two groups in phenotypes of the cells in the blast region of bone marrow. Group A showed higher percentages of B lymphoid cells in the blast region than did group B. There were no differences between the two groups in the percentages of $CD13^+$, $CD33^+$, $CD14^+$, $CD15^+$, $CD11b^+$, $CD11c^+$, $CD5^+$, $CD2^+$, $CD7^+$, $CD25^+$, $CD36^+$, $CD41^+$, $CD56^+$, $CD34^+$, $CD117^+$, and $HLA\text{-}DR^+$

Table I. Characteristics of the patients before receiving imatinib.

	Group A	Group B	*p*
Patient (no)	26	6	
Age (years)#	57 (19–75)	47.0 (31–55)	0.06
Gender (female/male, no)	17/9	5/1	
White blood cells ($10^3/\mu L$)*	41.5	47.1	0.423
Hemoglobin (g/dL)*	13.5	12	0.43
Platelets ($10^5/\mu L$)*	64.8	64.5	0.99
PB blasts (%)*	1	2.5	0.229
PB basophils (%)*	4.4	3.4	0.628
PB eosinophils (%)*	3	4.2	0.366
BM blasts (%)*	7.2	8.3	0.297
BM promyelocytes (%)*	8.4	5	0.224
BM myelocytes (%)*	16.5	14.3	0.489
BM metamyelocytes (%)*	4.6	5.4	0.724
BM bands (%)*	24.6	29.7	0.586
BM segmented neutrophils (%)*	22.9	24.6	0.711
Splenomegaly (cm)	25	6	0.667
Ph chromosome (%)	100	100	
Other chromosome (no)	1	0	0.812
Sokal score	0.8	0.9	0.411
Hasford score	799.1	884	0.638
Imatinib daily dose (mg)*	349	284.4	0.051

Spleen size was evaluated by ultrasonography.
no, number; PB, peripheral blood; BM, bone marrow; Ph, Philadelphia.
*Mean.

cells in the blast region. There was a significant difference between ratios of $CD33^+$ cell percentages to $CD10^+$ cell percentages in the two groups (Figure 1). Significant differences were found in CD33/CD19 ratios, CD13/CD10 ratios and CD13/CD19 ratios between the two groups (Figure 1). CD33/CD10, CD33/CD19, CD13/CD10 and CD13/CD19 ratios in the blast region distinguished clearly between the two groups. Cell compositions in the blast region in Group A were similar to those in MDS and healthy volunteers (Figure 1). After one year treatment of imatinib, bone marrow differentials were not different in the two groups: blasts, promyelocytes, myelocytes, metamyleocytes, bands and segmented neutrophils in Group A were 2.3, 2.3, 6.6, 4.2, 18.5 and 25.9%, respectively, whereas blasts, promyelocytes, myelocytes, metamyleocytes, bands and segmented neutrophils in Group B were 8.3, 2.3, 8.1, 2.3, 18.3 and 13.5%, respectively. Three of the six patients in Group B progressed to an accelerated phase. In contrast, none of the patients in group A progressed to an accelerated phase or blastic crisis. After six months of treatment with imatinib, CD33/CD10, CD33/CD19, CD13/CD10 and CD13/CD19 ratios in the blast region were lower in the group showing a CCyR (24 patients) than in the group not showing a CCyR (8 patients): 7.7 vs. 42.8 ($p < 0.05$), 7.5 vs. 18.7 ($p < 0.01$), 9.4 vs. 29.5 ($p = 0.06$) and 6.7 vs. 19.0 ($p < 0.05$), respectively. Molecular responses were evaluated after six months of treatment with imatinib: the group showing an undetectable number of BCR/ABL messages was designated as Group C (17 patients), and the group showing a detectable number of BCR/ABL messages was designated as Group D (9 patients). There were no differences between these two groups in peripheral blood cell counts, peripheral blood blast percentages, peripheral blood basophil percentages, bone marrow blast percentages, bone marrow differentials, size of splenomegaly and imatinib doses per day. CD33/CD10, CD33/CD19, CD13/CD10 and CD13/CD19 ratios in the blast region were lower in Group C than in Group D: 6.4 vs. 11.6 ($p = 0.05$), 6.1 vs. 10.5 ($p < 0.05$), 8.1 vs. 13.9 ($p < 0.05$) and 5.7 vs. 9.4 ($p < 0.05$), respectively.

Prognostic factors in CML at initial presentation have been reported to include bone marrow fibrosis, megakaryocyte number, bone marrow cellularity and basophil-lineage cells [9–12]. We showed that decrease in $CD19^+$ B lymphoid cells in the blast region is associated with a poor response to imatinib. Interestingly, cell compositions in the blast region in Group A of CML were similar to those in MDS and healthy volunteers. In our patients, neither Sokal scores nor Hasford scores predicted responses to imatinib. Sokal and Hasford scoring systems were

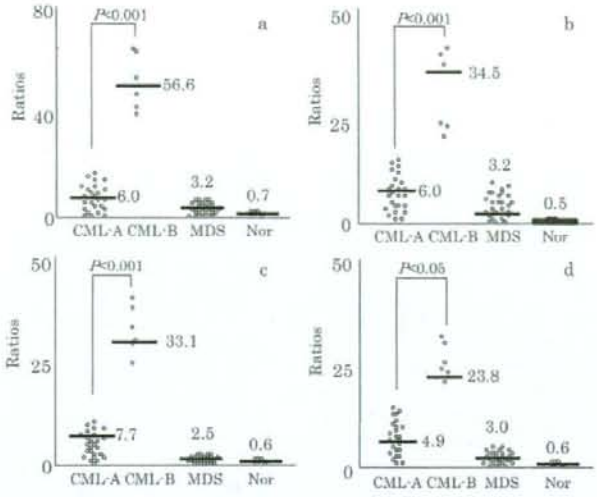

Figure 1. Ratios of antigen expression in the blast region of bone marrow. CML, chronic myelogeneous leukemia; CML-A, CML group showing a complete cytogenetic response (CCyR) after one-year treatment with imatinib; CML-B, CML group not showing a CCyR after the treatment; MDS, refractory anemia of myelodysplastic syndrome; Nor, healthy volunteer; a, CD33/CD10; b, CD33/CD19; c, CD13/CD10; d, CD13/CD19. The values are means.

established on the basis of non-specific laboratory and clinical parameters for CML patients receiving interferon or chemotherapy, respectively [13]. Therefore, cell compositions in the blast region of bone marrow may be directly related to the proliferation of CML progenitors, leading to response to imatinib. The FCM with a CD45/side-scatter gate used in this study separates immature cells including blasts from other cells in bone marrow. This FCM is superior to FCM with a forward scatter/side-scatter gate to identify small populations of the immature cells in bone marrow [6,7]. The FCM with a CD45/side-scatter gate is widely used for determining leukemia phenotypes as well as detecting minimal residual disease in leukemia as a routine practice in FCM laboratories at hospitals and laboratory companies. Therefore, physicians can order the analysis of immature cell phenotypes in the bone marrow in CML using FCM with a CD45/side-scatter gate. FCM has several advantages to polymerase chain reaction: results from FCM are obtained within one or two days and FCM data can be easily re-analysed if needed. Our results indicate that a cut-off value 30 of CD33/CD10 ratios in the blast region evaluated by FCM with a CD45/side-scatter gate in CML at diagnosis may be useful for the prediction of response to imatinib. According to our results, it is recommended that patients with CML at diagnosis showing more than this cut-off value should be carefully followed after the start of imatinib therapy. If Ph chromosome does not disappear by the end of one year of treatment with imatinib in these patients, other therapeutic options such as increased doses of imatinib and dasatinib or nioltinib instead of imatinib should be considered. These alternative therapies may lead to durable a CCyR in such patients.

Recently, imatinib trough levels in plasma have been shown to be associated with both cytogenetic and molecular responses to imatinib in patients with CML [14,15]. We did not measure imatinib trough levels in plasma in our patients. Further studies are needed to identify relationships between cell compositions in the blast region of bone marrow and imatinib trough levels in plasma in the response of CML to imatinib.

Acknowledgement

This study was supported by Jichi University Young Investigator Award.

References

1. Kavalerchik E, Goff D, Jamieson CH. Chronic myeloid leukemia stem cells. J Clin Oncol 2008;26:2911–2955.
2. Savage DG, Antman KH. Imatinib mesylate-a new oral targeted therapy. N Engl J Med 2002;346:683–693.
3. Druker BJ, Guilhot F, O'Brien SG, Gathmann I, Kantarjian H, Gattermann N, et al. Five-year follow-up of patients receiving imatinib for chronic myeloid leukemia. N Engl J Med 2006;355:2408–2417.